J|A|C|S ARTICLES

Published on Web 06/28/2010

Multidentate Poly(ethylene glycol) Ligands Provide Colloidal Stability to Semiconductor and Metallic Nanocrystals in Extreme Conditions

Michael H. Stewart,[†] Kimihiro Susumu,[†] Bing C. Mei,[†,§] Igor L. Medintz,[‡] James B. Delehanty,[‡] Juan B. Blanco-Canosa,[||] Philip E. Dawson,[||] and Hedi Mattoussi*[,†,⊥]

Optical Sciences Division and Center for Bio/Molecular Science and Engineering, Naval Research Laboratory, Washington, D.C. 20375, and Departments of Cell Biology & Chemistry and Skaggs Institute for Chemical Biology, The Scripps Research Institute, La Jolla, California 92037

Received April 6, 2010; E-mail: mattoussi@chem.fsu.edu

Abstract: We present the design and synthesis of a new set of poly(ethylene glycol) (PEG)-based ligands appended with multidentate anchoring groups and test their ability to provide colloidal stability to semiconductor quantum dots (QDs) and gold nanoparticles (AuNPs) in extreme buffer conditions. The ligands are made of a PEG segment appended with two thioctic acid (TA) or two dihydrolipoic acid (DHLA) anchoring groups, bis(TA)-PEG-OCH_3 or bis(DHLA)-PEG-OCH_3. The synthesis utilizes Michael addition to create a branch point at the end of a PEG chain combined with carbodiimide-coupling to attach two TA groups per PEG chain. Dispersions of CdSe−ZnS core−shell QDs and AuNPs with remarkable long-term colloidal stability at pHs ranging from 1.1 to 13.9 and in the presence of 2 M NaCl have been prepared and tested using these ligands. AuNPs with strong resistance to competition from dithiothreitol (as high as 1.5 M) have also been prepared. This opens up possibilities for using them as stable probes in a variety of bio-related studies where resistance to degradation at extreme pHs, at high electrolyte concentration, and in thiol-rich environments is highly desirable. The improved colloidal stability of nanocrystals afforded by the tetradentate ligands was further demonstrated via the assembly of stable QD−nuclear localization signal peptide bioconjugates that promoted intracellular uptake.

Introduction

A tremendous interest in inorganic nanocrystals such as gold nanoparticles (AuNPs) and semiconductor quantum dots (QDs) has been spurred by their unique size- and composition-tunable optical and spectroscopic properties.[1−5] This interest is motivated by the potentials they offer in a variety of applications, which include uses in electronic devices and cellular imaging and as biological sensors.[2−7] High-quality QDs are very attractive for many biological applications due to their broad absorption spectra, tunable emission, chemical stability, and resistance to photobleaching.[2,4,8] Luminescent QDs are reproducibly prepared with narrow size distributions and high fluorescence quantum yields by pyrolysis of organometallic precursors.[9] The resulting QDs are typically capped with hydrophobic molecules, which provide colloidal stability and solubility in hydrophobic organic solvents. Thus, post-synthetic surface modification is required to render these nanocrystals soluble and stable in buffer media and thus compatible with biological manipulations.

Several strategies have been reported for preparing water-soluble QDs starting from hydrophobic nanocrystals. One method, known as encapsulation, involves the use of phospholipids or amphiphilic polymers to encapsulate the as-made QDs in a micelle-like structure.[10−13] Another method, referred to as

[†] Optical Sciences Division, Naval Research Laboratory.
[‡] Center for Bio/Molecular Science and Engineering, Naval Research Laboratory.
[||] The Scripps Research Institute.
[§] Present address: Avon Products Inc., One Avon Place, Suffern, NY 10901-5605.
[⊥] Present address: Department of Chemistry, Florida State University, Tallahassee, FL 32306.

(1) Link, S.; El-Sayed, M. A. *Int. Rev. Phys. Chem.* **2000**, *19*, 409–453.
(2) Alivisatos, P. *Nat. Biotechnol.* **2004**, *22*, 47–52.
(3) Daniel, M. C.; Astruc, D. *Chem. Rev.* **2004**, *104*, 293–346.
(4) Medintz, I. L.; Uyeda, H. T.; Goldman, E. R.; Mattoussi, H. *Nat. Mater.* **2005**, *4*, 435–446.
(5) Sperling, R. A.; Rivera gil, P.; Zhang, F.; Zanella, M.; Parak, W. J. *Chem. Soc. Rev.* **2008**, *37*, 1896–1908.
(6) Raymo, F. M.; Yildiz, I. *Phys. Chem. Chem. Phys.* **2007**, *9*, 2036–2043.
(7) Kim, L.; Anikeeva, P. O.; Coe-Sullivan, S. A.; Steckel, J. S.; Bawendi, M. G.; Bulovic, V. *Nano Lett.* **2008**, *8*, 4513–4517.
(8) Michalet, X.; Pinaud, F. F.; Bentolila, L. A.; Tsay, J. M.; Doose, S.; Li, J. J.; Sundaresan, G.; Wu, A. M.; Gambhir, S. S.; Weiss, S. *Science* **2005**, *307*, 538–544.
(9) Murray, C. B.; Norris, D. J.; Bawendi, M. G. *J. Am. Chem. Soc.* **1993**, *115*, 8706–8715.
(10) Pellegrino, T.; Manna, L.; Kudera, S.; Liedl, T.; Koktysh, D.; Rogach, A. L.; Keller, S.; Radler, J.; Natile, G.; Parak, W. J. *Nano Lett.* **2004**, *4*, 703–707.
(11) Carion, O.; Mahler, B.; Pons, T.; Dubertret, B. *Nat. Protoc.* **2007**, *2*, 2383–2390.
(12) Yu, W. W.; Chang, E.; Falkner, J. C.; Zhang, J. Y.; Al-Somali, A. M.; Sayes, C. M.; Johns, J.; Drezek, R.; Colvin, V. L. *J. Am. Chem. Soc.* **2007**, *129*, 2871–2879.
(13) Lees, E. E.; Nguyen, T. L.; Clayton, A. H. A.; Mulvaney, P.; Muir, B. W. *ACS Nano* **2009**, *3*, 1121–1128.

 10.1021/ja102898d

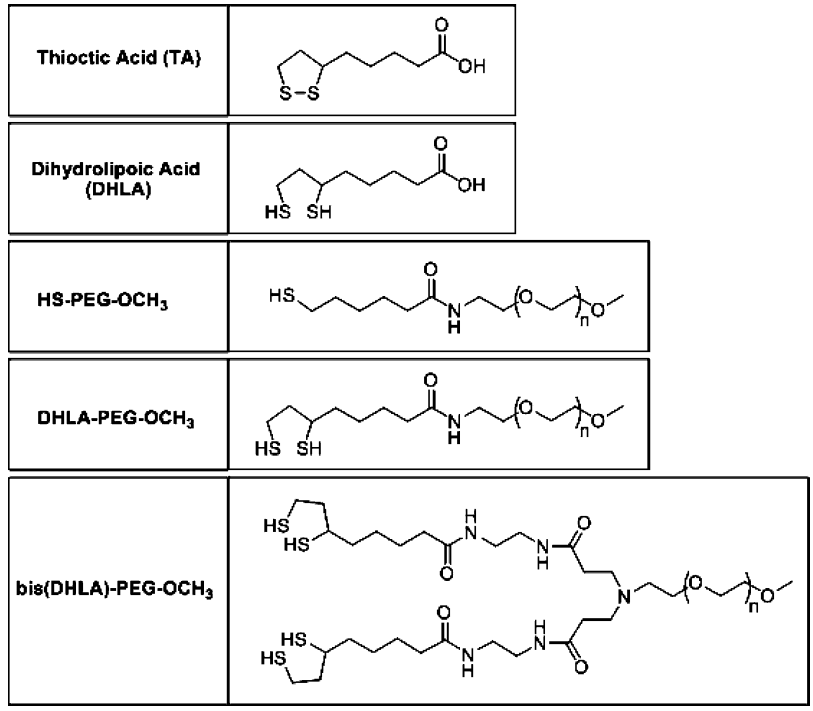

Figure 1. Structure of the PEG-appended ligands together with the disulfide precursor (PEG750 chain with $n \approx 15$). Only the reduced forms of the PEGylated ligands are shown.

cap exchange (or ligand exchange), involves replacing the hydrophobic cap with bifunctional hydrophilic ligands that contain a functional group for anchoring the ligand to the nanocrystal surface and a second module that promotes aqueous solubility.[14−19] Regardless of the method used, good colloidal stability is a prerequisite for developing nanoparticles with great potential utility in biology. In particular, preparing QDs that are stable in extreme buffers (strongly acidic and/or strongly basic) will allow processing them under harsh chemical conditions and will greatly expand their utility for biological labeling and tracking.

We find cap exchange beneficial because coating the nanocrystal surface with tailor-made ligands provides QDs with small hydrodynamic diameters and permits the introduction of specific functionalities for further coupling and modification.[4,8,20] These two criteria are crucial for interfacing the nanocrystals with biological systems and tailoring them to desired applications.[4] The success of these applications is highly dependent on the QDs maintaining colloidal stability, which is largely determined by the nature of the ligands used to cap the nanocrystals' surface. There are two important variables inherent to the ligands that greatly influence the stability of the hydrophilic QDs: (1) the affinity of the anchoring group to the inorganic surface and (2) how aqueous solubility is achieved (i.e., via electrostatic repulsions between surface charges or strong ligand affinity to the surrounding solvent).

We and other groups have shown that QDs capped with dithiol ligands, such as dihydrolipoic acid (DHLA, Figure 1), are more stable than those capped with monothiol ligands, which is attributed to an increased affinity of dithiol ligand to the nanocrystal surface.[14−16] DHLA is obtained by reduction of the dithiolane ring of commercially available thioctic acid (TA, Figure 1). The enhanced binding of multidentate, thiol-chelating ligands to Au surfaces and the concomitant effect of increasing Au nanoparticle stability have also been well documented.[21−24] We have also shown that better colloidal stability is achieved when a poly(ethylene glycol) (PEG) segment is appended onto the anchoring group. For instance, DHLA-PEG-OCH_3 ligands (shown in Figure 1) promote aqueous compatibility of QDs in buffered solutions from pH 4 to pH 11, and significantly reduce nonspecific interactions in biological conditions;[15,17] other independent studies have also shown that functionalizing QDs with PEGylated coating can reduce nonspecific interactions.[25] Furthermore, PEG-appended TA or DHLA ligands were shown to provide excellent colloidal stability to AuNPs as well.[17,26] These findings combined indicate that ligands containing

(14) Mattoussi, H.; Mauro, J. M.; Goldman, E. R.; Anderson, G. P.; Sundar, V. C.; Mikulec, F. V.; Bawendi, M. G. *J. Am. Chem. Soc.* **2000**, *122*, 12142–12150.
(15) Susumu, K.; Uyeda, H. T.; Medintz, I. L.; Pons, T.; Delehanty, J. B.; Mattoussi, H. *J. Am. Chem. Soc.* **2007**, *129*, 13987–13996.
(16) Liu, W.; Howarth, M.; Greytak, A. B.; Zheng, Y.; Nocera, D. G.; Ting, A. Y.; Bawendi, M. G. *J. Am. Chem. Soc.* **2008**, *130*, 1274–1284.
(17) Mei, B. C.; Susumu, K.; Medintz, I. L.; Delehanty, J. B.; Mountziaris, T. J.; Mattoussi, H. *J. Mater. Chem.* **2008**, *18*, 4949–4958.
(18) Susumu, K.; Mei, B. C.; Mattoussi, H. *Nat. Protoc.* **2009**, *4*, 424–436.
(19) Poselt, E.; Fischer, S.; Foerster, S.; Weller, H. *Langmuir* **2009**, *25*, 13906–13913.
(20) Pons, T.; Uyeda, H. T.; Medintz, I. L.; Mattoussi, H. *J. Phys. Chem. B* **2006**, *110*, 20308–20316.
(21) Li, Z.; Jin, R. C.; Mirkin, C. A.; Letsinger, R. L. *Nucleic Acids Res.* **2002**, *30*, 1558–1562.
(22) Park, J. S.; Vo, A. N.; Barriet, D.; Shon, Y. S.; Lee, T. R. *Langmuir* **2005**, *21*, 2902–2911.
(23) Srisombat, L. O.; Park, J. S.; Zhang, S.; Lee, T. R. *Langmuir* **2008**, *24*, 7750–7754.
(24) Zhang, S. S.; Leem, G.; Srisombat, L. O.; Lee, T. R. *J. Am. Chem. Soc.* **2008**, *130*, 113–120.
(25) Bentzen, E. L.; Tomlinson, I. D.; Mason, J.; Gresch, P.; Warnement, M. R.; Wright, D.; Sanders-Bush, E.; Blakely, R.; Rosenthal, S. J. *Bioconjugate Chem.* **2005**, *16*, 1488–1494.
(26) Mei, B. C.; Oh, E.; Susumu, K.; Farrell, D.; Mountziaris, T. J.; Mattoussi, H. *Langmuir* **2009**, *25*, 10604–10611.

Scheme 1. Synthesis of Chelating Ligands and Intermediates

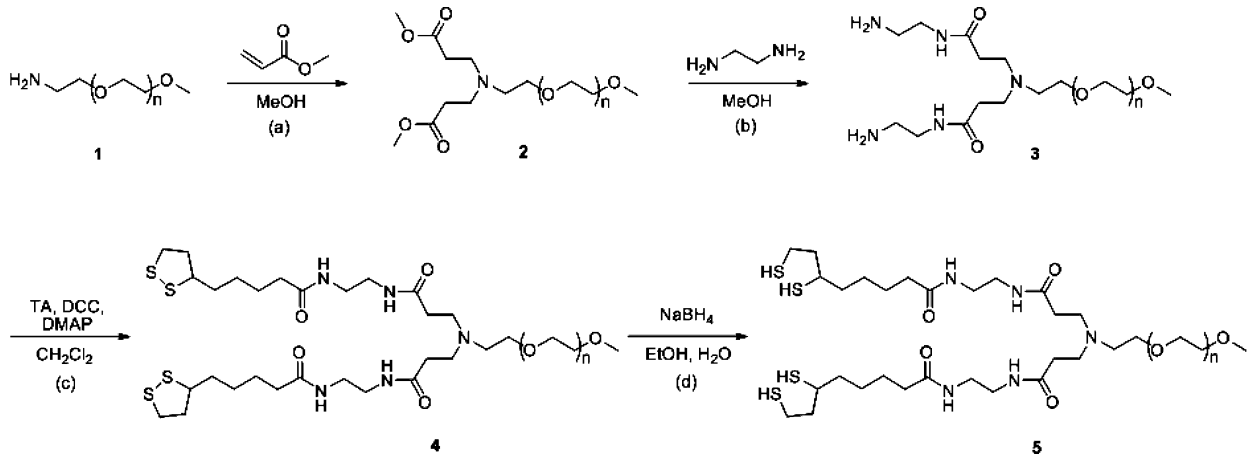

multiple thiols per anchoring group and a hydrophilic PEG module can provide improved colloidal stability to nanocrystals in aqueous media.

In this report, we build on those results and present the design and synthesis of new modular PEG-based ligands that contain two dithiolane or two DHLA anchoring groups (i.e., bis(TA)-PEG-OCH_3 (**4**) and bis(DHLA)-PEG-OCH_3 (**5**), see Figure 1 and Scheme 1). This design is inspired by the wealth of work on dendrimers and uses Michael addition to introduce multiple anchoring groups onto a single PEG chain, which enhances the ligand affinity to the inorganic surfaces of nanocrystals. As a result, we have prepared QDs and AuNPs capped with tetrathiol ligands that exhibit remarkable pH stability and improved resistance to aggregation compared to nanocrystals capped with monothiol- and dithiol-terminated analogues. Stability of the nanocrystals was further demonstrated via bioconjugation to nuclear localization signal (NLS) peptides and subsequent aggregation-free uptake by COS-1 cells.

Results and Discussion

Synthesis. Our design was motivated by previous observations that ligands presenting two coordinating groups provide improved colloidal stability to QDs and AuNPs than their monovalent counterparts and the ability of PEG moieties to promote excellent water and biological compatibility. For instance, we have shown that DHLA-PEG ligands containing two thiols per anchoring group provide improved colloidal stability to QDs and AuNPs in the presence of electrolytes and to changes in the solution pH (compared to analogous ligands containing a single thiol).[15,17,26] The DHLA-PEG ligands were made by appending one TA group to H_2N-PEG-OCH_3 via carbodiimide coupling with *N*,*N*′-dicyclohexylcarbodiimide (DCC) followed by reduction of the dithiolane ring with $NaBH_4$.[15,17] Thus, anchoring groups with higher coordination (e.g., two DHLA groups with four thiols) will provide additional stability to the ligand−nanocrystal binding. To attach an anchoring group containing multiple DHLA groups on a PEG segment, we were inspired by an elegant branching strategy developed for the synthesis of dendrimers and other hyperbranched polymers,[27] where a single amine group at the PEG terminus is branched into two amines via Michael addition with methyl acrylate followed by amidation with ethylenediamine (EDA) (see steps a and b, Scheme 1). The two amines introduced with this branching motif accommodate the attachment of two TA groups per PEG moiety. This strategy was utilized to synthesize the multidentate ligands bis(TA)-PEG-OCH_3 and bis(DHLA)-PEG-OCH_3 (**4** and **5**, respectively) and their intermediates using a stepwise approach (Scheme 1).

First, commercially available poly(ethylene glycol) methyl ether (HO-PEG-OCH_3, average MW $\approx$ 750, $n \approx 15$) was transformed to H_2N-PEG-OCH_3 (**1**) as we previously reported.[17] Next, alkylation of the amine with methyl acrylate via Michael addition was used to introduce a Y-shaped branching point at the terminus of the PEG chain to yield **2** (Scheme 1, step a); using excess methyl acrylate ($\sim$11:1) increases the efficiency of the transformation. The alkylation step is critical because the branch provides two methyl ester groups per PEG that can be further modified. Moreover, this step (Michael addition) is relatively simple, and the product (**2**) is easy to isolate in high yield ($\sim$80%). Amidation of the methyl ester groups with excess EDA (step b) produces two reactive amine groups per PEG chain (**3**). Stirring the reaction mixture for 4 days with a large excess of EDA ($\sim$200 equiv) ensures complete amidation of the methyl ester groups. However, removal of all EDA from the reaction mixture (via thorough evaporation under reduced pressure) is critical before proceeding to the next step (step c). Trace amounts of EDA left mixed with compound **3** (in step c) can competitively consume TA during the DCC coupling reaction, ultimately reducing the yield of bis(TA)-PEG-OCH_3 (**4**). Coupling of the two amines of compound **3** to TA in the presence of DCC and dimethylaminopyridine (DMAP) is simple and highly efficient, and the product (**4**) can be purified by column chromatography. Additional details on the synthesis of the various compounds are provided in the Supporting Information.

Bis(TA)-PEG-OCH_3 (**4**) can be used directly for capping AuNPs without the need for reducing the dithiolane rings. For QDs, however, reduction of the dithiolane rings with $NaBH_4$ to produce thiol groups (bis(DHLA)-PEG-OCH_3 (**5**)) is required for coordination onto the semiconductor surfaces (step d).[14] One key advantage of the ligand design is that a single synthetic pathway is used to provide higher coordination ligands for both AuNPs and QDs.

We should emphasize that, in principle, steps a and b in the transformation can be repeated prior to the final DCC coupling with TA to provide a highly branched ligand structure containing

(27) Tomalia, D. A.; Baker, H.; Dewald, J.; Hall, M.; Kallos, G.; Martin, S.; Roeck, J.; Ryder, J.; Smith, P. *Macromolecules* **1986**, *19*, 2466–2468.

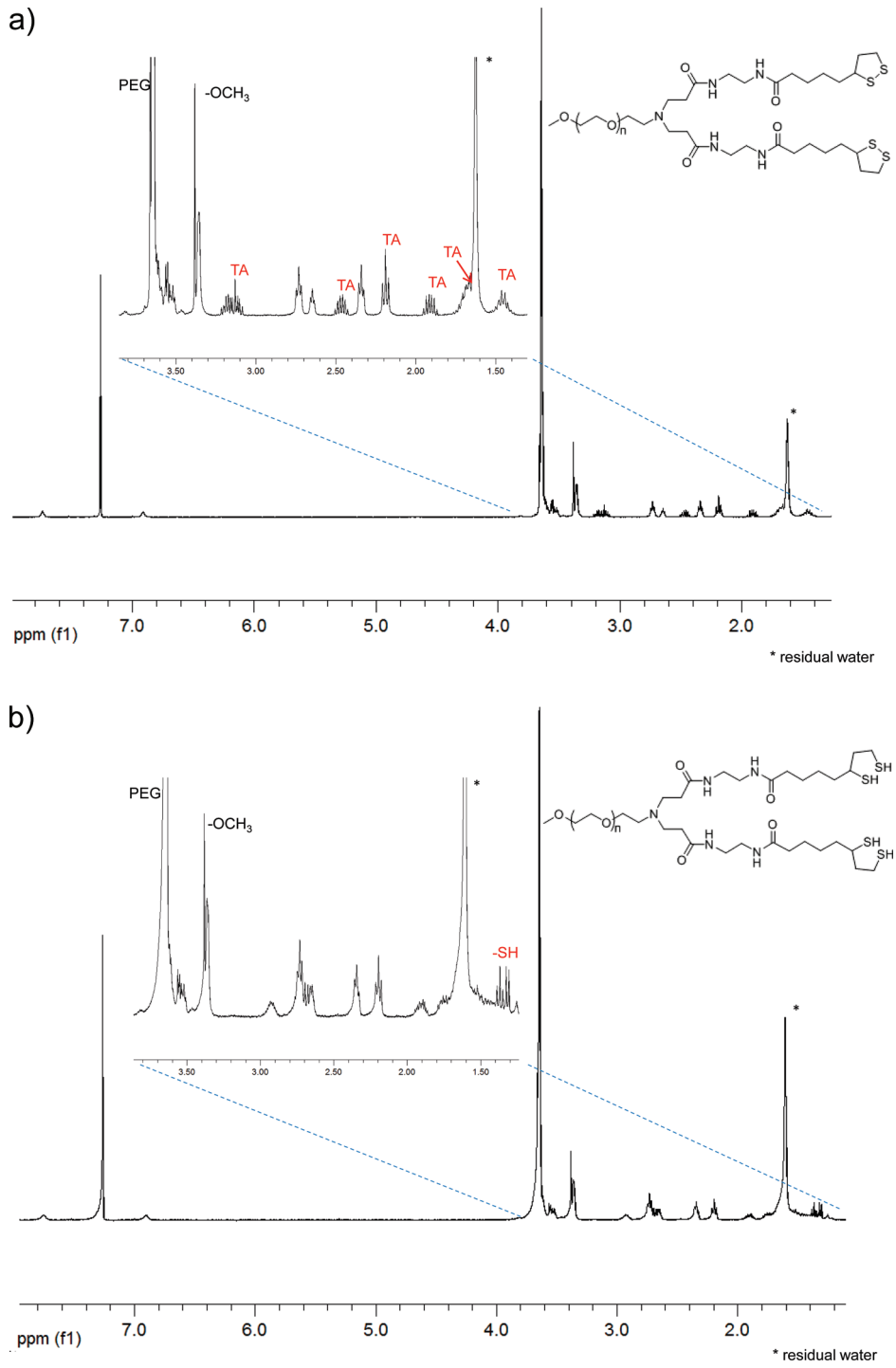

Figure 2. ^{1}H NMR spectra of compounds **4** (top) and **5** (bottom). The signature of the PEG chain is maintained in both spectra, while reduction of the dithiolane groups is reflected in the well-resolved triplet and doublet peaks at 1.37 and 1.32 ppm, respectively.

multiple amine groups per PEG segment, i.e., 2^n amines, with n being the number of iterations used. The amine groups could then be DCC-coupled to TA to provide 2^n TA groups per PEG chain and 2^{n+1} thiol groups per PEG chain when reduced. Clearly, this synthetic pathway can provide a large and controllable number of thiol groups appended onto a single PEG chain.

Characterization of the final products and intermediates was carried out using ^{1}H NMR spectroscopy (Figure 2 and Supporting Information). Conveniently, compound **1** contained a single methoxy group (3.38 ppm, singlet) that provided an integration handle for monitoring and confirming successive, stepwise transformations on the NH_2 end of the PEG chain. In particular, the ^{1}H NMR spectrum of compound **2** (Supporting Information, Figure S1) showed methylene ($-CH_2-$) resonances at 2.82 (triplet) and 2.46 ppm (triplet), indicating that two methyl acrylate molecules were attached to the NH_2 group of compound **1**. Subsequent treatment with EDA yielded compound **3** and the ^{1}H NMR spectrum (Supporting Information, Figure S2), which displays two additional methylene resonances with integrations that confirm two EDA molecules per PEG chain. The ^{1}H NMR spectrum of compound **4** (Figure 2A) is a

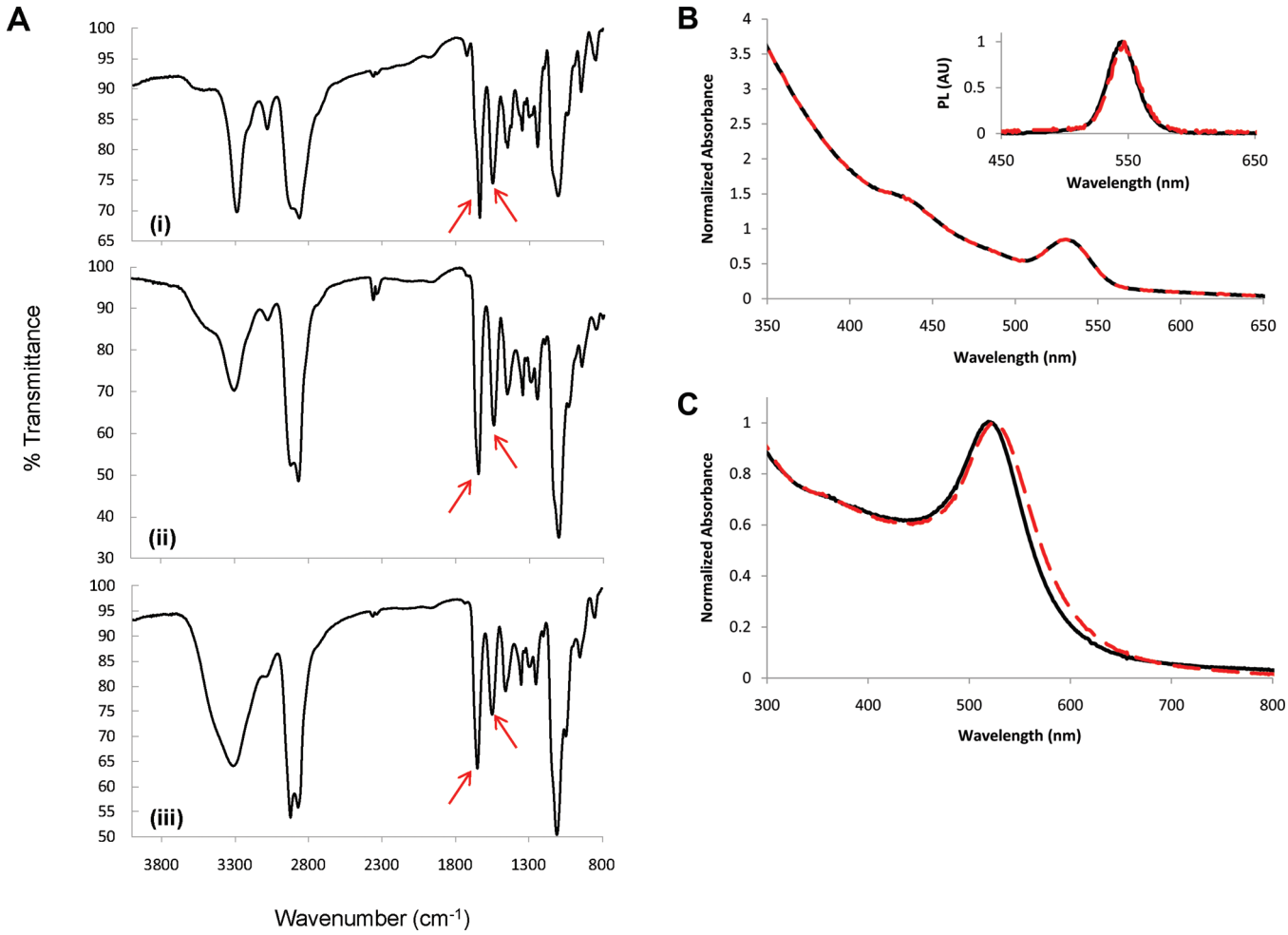

Figure 3. (A) FT-IR spectra of (i) bis(TA)-PEG-OCH_3, (ii) bis(TA)-PEG-OCH_3-capped AuNPs, and (iii) bis(DHLA)-PEG-OCH_3-capped QDs. (B) Absorption and fluorescence (inset) spectra of QDs capped with TOP/TOPO ligands in toluene (solid black line) and QDs capped with bis(DHLA)-PEG-OCH_3 (dashed red line). (C) Absorption spectra of commercially available 15 nm AuNPs stabilized with citric acid (solid black line) and cap-exchanged with bis(TA)-PEG-OCH_3 (dashed red line).

composite of those collected from TA and compound **3**. Comparing the relative integrations of the TA resonances and the PEG-methoxy resonance confirms the attachment of two TA groups per PEG. Upon reduction, the thiol protons of compound **5** (Figure 2B) are clearly reflected by the well-resolved triplet and doublet at 1.37 and 1.32 ppm.[15] Furthermore, the presence of two DHLA groups per PEG chain was confirmed by integration of the ^{1}H NMR spectrum.

Cap Exchange. We used CdSe−ZnS core−shell QDs (λ_{em} = 530 and 545 nm) and CdSe−CdZnS−ZnS core−shell−shell (λ_{em} = 630 nm) QDs that were synthesized according to previously published procedures via pyrolysis of organometallic precursors.[9,28,29] Cap exchange of the native hydrophobic ligands on the QDs with bis(DHLA)-PEG-OCH_3 effectively promoted transfer of the QDs to aqueous media over a broad range of pH (see below). The FT-IR spectrum of the free ligand bis(TA)-PEG-OCH_3 matched the one measured for the QDs after cap exchange (Figure 3A). Specifically, the characteristic sharp bands at 1643 cm^{-1} for the amide I (C═O stretch) and 1539 cm^{-1} for the amide II (N−H bending) of the PEG ligands were present in the spectra of the cap-exchanged QDs. Furthermore, the absorption and emission spectral profiles for the aqueous QDs capped with bis(DHLA)-PEG-OCH_3 were identical to those collected for the hydrophobic QDs dispersed in toluene (Figure 3B). These results also indicate that cap exchange with bis(DHLA)-PEG-OCH_3 does not result in deterioration of the inorganic cores of the QDs. A reduction in the photoluminescence (PL) quantum yield (by ∼50%) was observed, which has been known when thiol-based ligands are assembled on the surface of CdSe−ZnS and in particular CdSe core only or CdS-overcoated QDs.[30−32] The quantum yields measured for these newly capped QDs were ∼15−30%; these values are comparable to those reported for CdSe−ZnS QDs capped with DHLA-PEG ligands.[15,30]

Similarly, effective cap exchange of citrate-stabilized AuNPs with bis(TA)-PEG-OCH_3 was verified by FT-IR spectroscopy (Figure 3A), with essentially identical FT-IR spectra collected for free bis(TA)-PEG-OCH_3 and for AuNPs after cap exchange with the same ligands. The distinct, sharp amide I (C═O stretch)

(28) Clapp, A. R.; Goldman, E. R.; Mattoussi, H. *Nat. Protoc.* **2006**, *1*, 1258–1266.
(29) Xie, R. G.; Kolb, U.; Li, J. X.; Basche, T.; Mews, A. *J. Am. Chem. Soc.* **2005**, *127*, 7480–7488.
(30) Uyeda, H. T.; Medintz, I. L.; Jaiswal, J. K.; Simon, S. M.; Mattoussi, H. *J. Am. Chem. Soc.* **2005**, *127*, 3870–3878.
(31) Bullen, C.; Mulvaney, P. *Langmuir* **2006**, *22*, 3007–3013.
(32) Munro, A. M.; Plante, I. J. L.; Ng, M. S.; Ginger, D. S. *J. Phys. Chem. C* **2007**, *111*, 6220–6227.

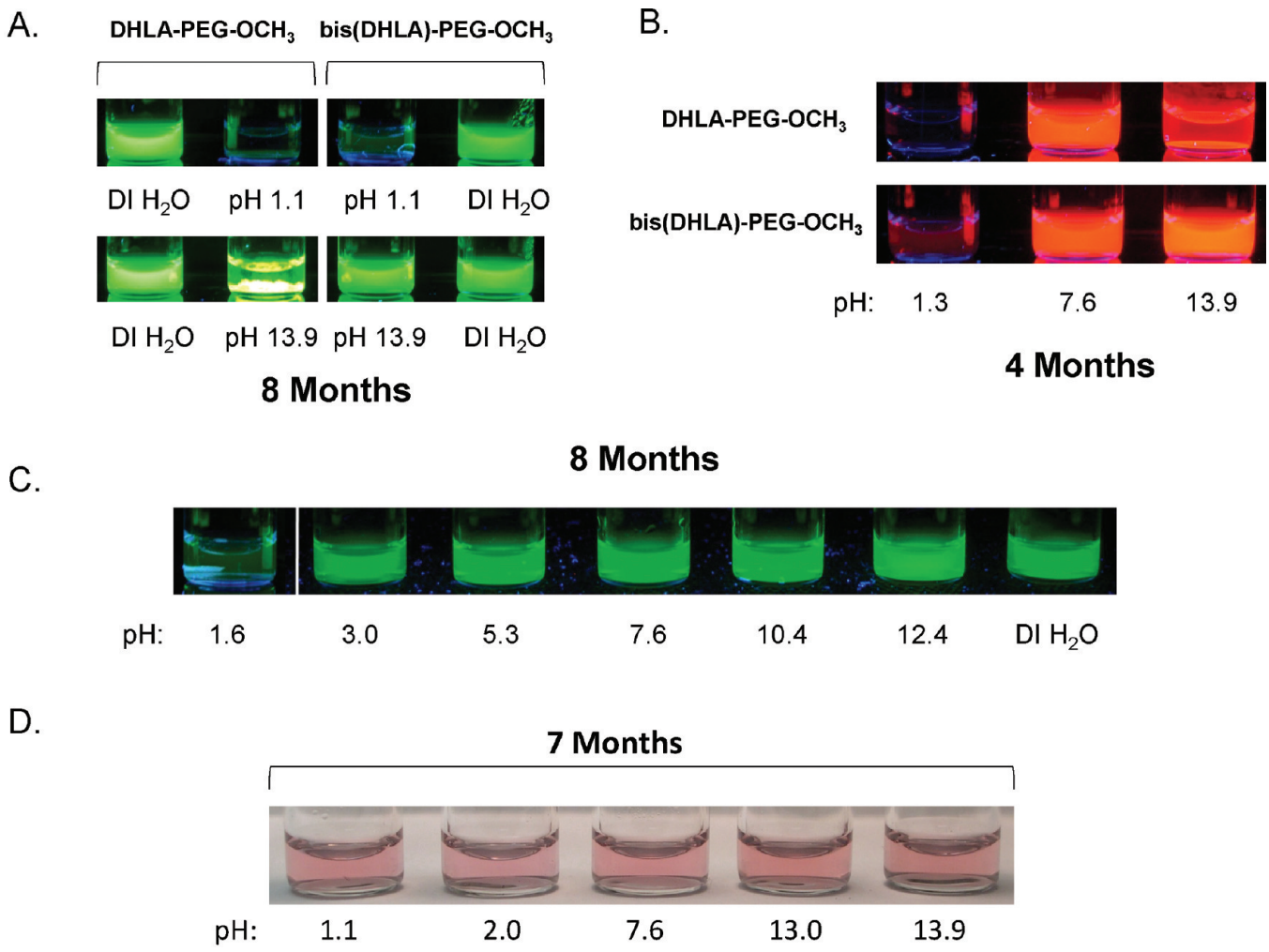

Figure 4. (A) Fluorescence images of CdSe−ZnS QDs (λ_{em} = 545 nm) capped with DHLA-PEG-OCH_3 (four vials on the left) and bis(DHLA)-PEG-OCH_3 (four vials on the right) after storage for 8 months at pH 1.1 and pH 13.9. Control samples in DI H_2O are also shown. (B) Fluorescence images of CdSe−CdZnS−ZnS QDs (λ_{em} = 630 nm) capped with DHLA-PEG-OCH_3 (top row) and bis(DHLA)-PEG-OCH_3 (bottom row) after 4 months of storage. The vials contain QDs in ∼1× PBS at the pH values 1.3, 7.6, and 13.9. (C) Fluorescence images of CdSe−ZnS QDs (λ_{em} = 545 nm) capped bis(DHLA)-PEG-OCH_3 at several pHs after 8 months of storage. A control sample in DI H_2O is also shown. All vials contain a QD concentration of ∼0.5 μM. (D) Image of AuNPs capped with bis(TA)-PEG-OCH_3 stored for 7 months in ∼1× PBS at the pH values listed below the vials. The nanoparticle concentration is ∼1 nM.

and amide II (N−H bending) bands at 1645 and 1539 cm^{-1}, respectively, of the PEG ligands were present in both spectra. The absorption spectra of the AuNPs before and after cap exchange with bis(TA)-PEG-OCH_3 were similar, which indicates that the PEG moiety of bis(TA)-PEG-OCH_3 promoted water dispersion without affecting the integrity of the AuNPs (Figure 3C). TEM images also revealed that cap exchange with bis(TA)-PEG-OCH_3 does not result in deterioration of the inorganic core via etching (Supporting Information, Figure S3). Given the strong similarities between TA (and DHLA) and bis(TA) (and bis(DHLA)) appended ligands (they both have the same PEG module), the hydrodynamic sizes for nanocrystals capped with either set of ligands should be similar and comparable to those measured for QDs and AuNPs capped with DHLA-PEG ligands. A detailed comparison between our DHLA-PEG-capped QDs and those prepared using various surface-functionalization strategies including commercial QDs were reported in ref 20.

Colloidal Stability of QDs and AuNPs to pH and Excess Electrolytes. We probed the effects of pH changes, added excess electrolytes (namely NaCl), and competitive ligand displacement by the small molecule dithiothreitol (DTT). Thus far, we have shown that the bidentate DHLA-PEG-based ligands can provide long-term colloidal stability (several months) to QDs in buffered solutions from pH 4 to pH 11.[17] A slightly broader pH range (3−12) was achieved for AuNPs capped with these ligands.[17] We therefore focused on testing the stability of nanocrystals under rather extreme conditions, including the stability of QDs capped with bis(DHLA)-PEG-OCH_3 or AuNPs capped with bis(TA)-PEG-OCH_3 at pH 1.1−2 (highly acidic) and pH 13.0−13.9 (highly basic) and in the presence of 2 M NaCl. Buffers at the desired pHs were prepared by adding a few drops of HCl or NaOH to 1× PBS stock solutions. Small volumes of the nanoparticles (after ligand exchange) were added to the buffers to yield solutions with final nanoparticle concentrations of ∼0.5 μM and ∼1 nM for the QDs and AuNPs, respectively. Nanocrystals capped with DHLA-PEG-OCH_3 or TA-PEG-OCH_3 were used for comparison.

Figure 4 shows a side-by-side comparison of the fluorescence images collected from two sets of dispersions in 1× PBS buffers after several months of storage in a refrigerator (at ∼5 °C and no extended exposure to light): green-emitting CdSe−ZnS QDs (λ_{em} = 545 nm) capped with bis(DHLA)-PEG-OCH_3 and DHLA-PEG-OCH_3 at pH 1.1 and pH 13.9 (Figure 4A) and red-

emitting CdSe−CdZnS−ZnS QDs (λ_{em} = 630 nm) capped with bis(DHLA)-PEG-OCH_3 and DHLA-PEG-OCH_3 at pH 1.3, 7.6, and 13.9 (Figure 4B). In addition, a set of green QD dispersions at several pHs ranging from pH 1.6 to pH 12.4 are also shown in Figure 4C. Clearly, the QDs capped with bis(DHLA)-PEG-OCH_3 maintained colloidal stability over several months at pH 1.1−1.3 and pH 13.9, with no sign of macroscopic aggregation in either set. Conversely, dispersions of nanocrystals capped with DHLA-PEG-OCH_3 showed poor colloidal stability at these harsh pH conditions, with observed aggregates and/or loss of fluorescence (Figure 4A). The DHLA-PEG-OCH_3-capped QDs at the extreme pHs precipitated rather rapidly: after 1.5 h at pH 1.1 and after 6 days at pH 13.9.

The fluorescence from dispersions of bis(DHLA)-PEG-capped QDs was essentially unchanged throughout the pH range from 3 to 13.9, as bright PL was observed for those pHs after several months of storage (Figure 4A−C). However, dimming of the solution emission was recorded for both set of QDs at pH 1−2; dimming occurred at ∼1.5 h after transfer, but emission stabilized for several months after the initial drop. The new higher coordination ligands also provided added colloidal stability in the presence of excess salt. We found that dispersions of QDs cap-exchanged with bis(DHLA)-PEG-OCH_3 were stable in the presence of 2 M NaCl for at least 8 months, with no signs of aggregation or loss of fluorescence (see Supporting Information, Figure S4).

Similarly, AuNPs capped with bis(TA)-PEG-OCH_3 showed excellent long-term stability to pH changes. An image of AuNPs dispersed in 1× PBS buffers at pH 1.1, 2.0, 7.6, 13, and 13.9 after 7 months of storage in a refrigerator is shown in Figure 4D. No visible sign of aggregation (usually manifesting in changes in the solutions color from red-pink to a purple-blue hue) was observed over the entire pH range.[33] The AuNP dispersions were also stable in 2 M NaCl for at least 7 months, as observed for QD dispersions above.

The enhanced ligand affinity to the AuNP surfaces was further tested in the presence of strong competition by the small molecule DTT. We have previously used DTT competition tests to probe differences in the stability of AuNPs cap-exchanged with HS-PEG-OCH_3 (shown in Figure 1) and TA-PEG-OCH_3 ligands.[26] Similar experiments have also been used by other groups to compare how well different ligand architectures stabilize AuNPs.[21,34] DTT is a dithiol reducing agent that is frequently used to prevent oxidation of cysteine in biomolecules.[35] At high concentrations, DTT can displace weakly to modestly bound ligands from the surface of AuNPs, inducing progressive aggregation; this process can be further accelerated in the presence of excess NaCl. Thus, the degree of AuNP stability imparted by a specific thiol-terminated ligand can be reflected in the kinetics of DTT-induced AuNP aggregation (i.e., weakly capped NPs become unstable with a fast rate of aggregation, whereas strongly bound ligands produce nanoparticles that exhibit very slow rates of aggregation).

DTT-induced aggregation of the AuNPs can be monitored by following the progressive changes in the absorption spectra, namely a decrease in the surface plasmon resonance band (SPB) combined with an increase in absorbance at longer wavelengths. This process can be quantified by monitoring changes in the aggregation factor (AF), defined as the ratio between the optical density at 615 nm and at the SPB (∼524 nm).[26,33] The absorption spectra of strongly capped and stable NPs will either remain unchanged or show minor perturbations with time (no or small changes in the AF, respectively). Conversely, if the capping ligands are weakly bound, AuNPs become unstable upon addition of DTT, and the AF will increase with time.

Figure 5A−C shows the time evolution (over a period of 60 min) of the absorption spectra collected for AuNPs capped with HS-PEG-OCH_3, TA-PEG-OCH_3, and bis(TA)-PEG-OCH_3, respectively, in aqueous solutions containing 1.5 M DTT (large excess) and 400 mM NaCl. The corresponding time-dependent change in the normalized aggregation factors is shown in Figure 5D. AuNPs capped with bis(TA)-PEG-OCH_3 showed excellent colloidal stability, with no signs of aggregation after 60 min. In contrast, significant aggregation was measured for dispersions of AuNPs capped with HS-PEG-OCH_3, as reflected by the rapid increase of the AF after 10 min. The AuNPs capped with TA-PEG-OCH_3, in comparison, exhibited weaker stability against competition by DTT than that recorded with bis(TA)-PEG-OCH_3, as reflected in the slight increase in AF over time; nanoparticle stability was still substantially better than what was achieved with HS-PEG-OCH_3.[26] Such DTT tests were not applied to QD dispersions because those do not exhibit changes in the absorption spectra as for AuNPs.

We should note that estimates of the overall number/density of ligands per nanoparticle cannot be carried out using the present set of multidentate ligands due to a lack of end reactive groups. We will carry out such experiments once the design of such a ligand is complete. We have, however, carried out ligand counting experiments using AuNPs capped with maleimide-modified TA-PEG ligands.[36] In that design we took advantage of the specific and highly efficient maleimide-to-cysteine reaction, combined with the ability of performing maleimide transformation on the ligand prior to cap exchange, and carried out ligand counting using dye-labeled, cysteine-terminated peptides. The ligand densities were extracted from absorption data collected for dispersions of NPs capped with varying fractions of TA-PEG-maleimide mixed with "inert" TA-PEG-OCH_3.[36] An average footprint area per ligand of 1.25 nm^2 was measured for these ligands, independent of the AuNP size used.

Combined, these results unequivocally demonstrate that aqueous dispersions of nanocrystals surface-capped with bis-(DHLA)-PEG-OCH_3 have substantially enhanced colloidal stability compared to those coated with monothiol- as well as dithiol-appended PEG ligands. Coordination of both ligands, bis(DHLA)-PEG-OCH_3 onto QDs and bis(TA)-PEG-OCH_3 onto AuNPs, is driven by the multidentate anchoring group, which provides more stable ligand-to-nanocrystal interactions and results in enhanced colloidal stability compared to their lower coordination counterparts. We should stress that both TA- and DHLA-appended ligands efficiently coordinate onto AuNPs, though only TA-appended ligands were tested in this study.[26] The increased affinity for higher coordination ligands derives from the nature of the thiol-to-metal interactions. The Zn-to-thiol or Au-to-thiol bond is not covalent (Lewis acid−base interactions) and can thus be affected by intermittent dissociation ("on" and "off" binding). Thus, a higher order of coordination will drastically reduce the probability of dissociation of the ligand (via the chelate effect), ultimately producing enhanced

(33) Zhao, W.; Brook, M. A.; Li, Y. F. *ChemBioChem* **2008**, *9*, 2363–2371.
(34) Dougan, J. A.; Karlsson, C.; Smith, W. E.; Graham, D. *Nucleic Acids Res.* **2007**, *35*, 3668–3675.
(35) Cleland, W. W. *Biochemistry* **1964**, *3*, 480–482.
(36) Oh, E.; Susumu, K.; Blanco-Canosa, J. B.; Medintz, I. L.; Dawson, P. E.; Mattoussi, H. *Small* **2010**, *6*, 1273–1278.

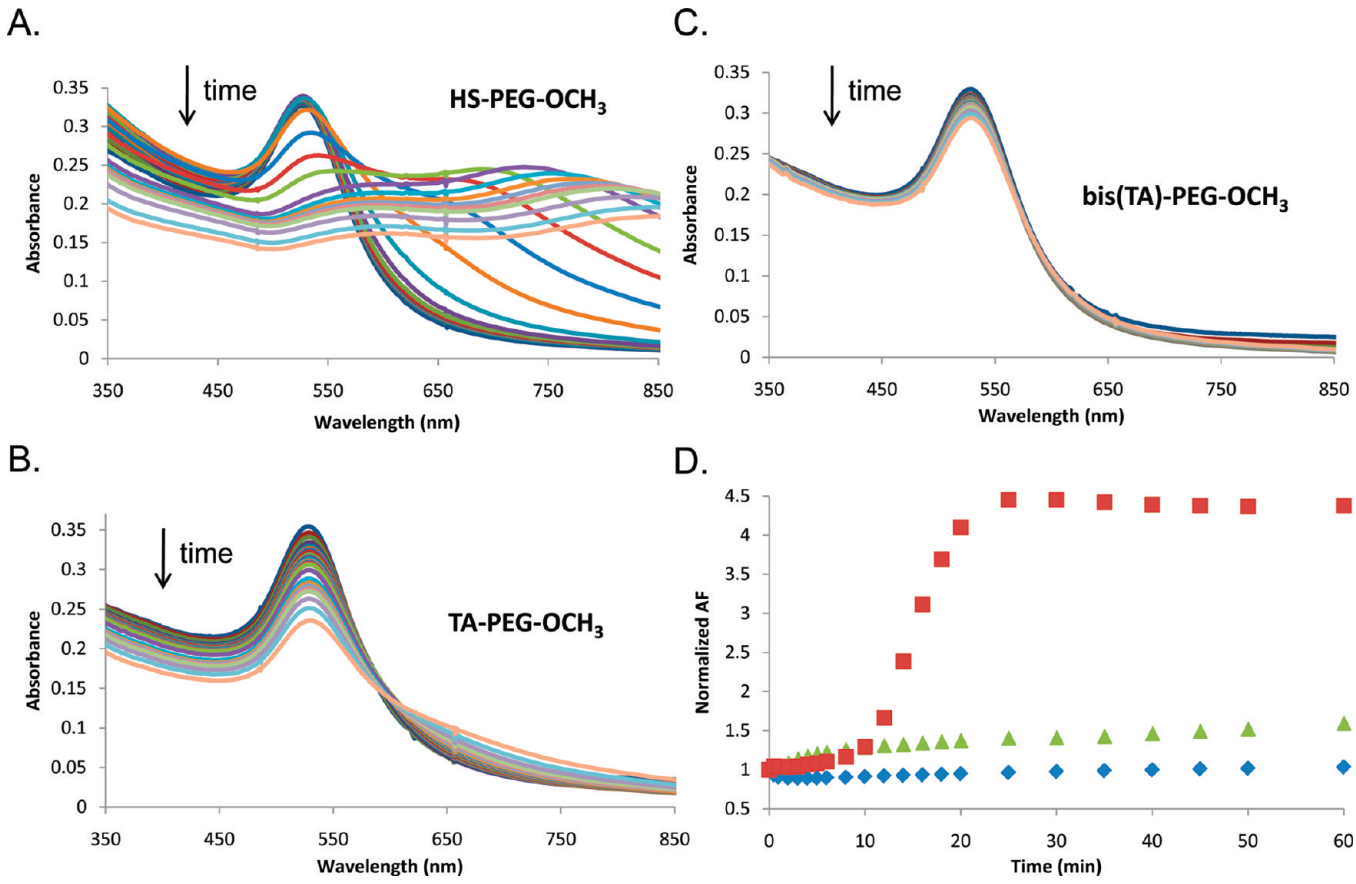

Figure 5. Time-dependent absorption spectra of AuNPs capped with (A) HS-PEG-OCH_3, (B) TA-PEG-OCH_3, and (C) bis(TA)-PEG-OCH_3 from 0 to 60 min in the presence of 1.5 M DTT and 400 mM NaCl with an initial OD (optical density) $\approx$ 0.33−0.35. (D) Plot of the normalized aggregation factors (AF) extracted from plots A, B, and C; HS-PEG-OCH_3 (red squares), TA-PEG-OCH_3 (green triangles), and bis(TA)-PEG-OCH_3 (blue diamonds).

affinity to the nanocrystal. Increasing the number of thiol groups per PEG chain from 1 (for HS-PEG-OCH_3) to 2 (for DHLA-PEG-OCH_3) to 4 (for bis(DHLA)-PEG-OCH_3) greatly enhances the stability of the PEG-capped nanocrystals.

QD Conjugation to Peptides and Cellular Uptake. Dispersions of nanoparticles surface-stabilized with these ligands have great potential utility for live cell and other *in vivo* studies. Effective coupling of NLS-containing peptides as well as cell penetrating peptides (CPP) to nanoparticles is critical to their use in cellular staining and sensing.[37] NLS peptides have been used for trafficking materials into the nucleus through signal-mediated pathways.[38] Thus, when controllably coupled to nanocrystals, these peptides should, upon delivery, be capable of targeting the nuclei of cells.[39−42]

We have shown that metal-affinity-driven self-assembly between several polyhistidine-appended peptides and CdSe−ZnS QDs capped with either DHLA or DHLA-PEG ligands provide functional QD−peptide conjugates; these conjugates were also used in intracellular uptake and imaging.[43] We have, however, found that coupling of polyhistidine-appended NLS peptides to DHLA-PEG-QDs often produced aggregates when high peptide-to-QD ratios were used, a result that we attribute to the high charge density of the peptides (see below). Given the remarkable stability exhibited by bis(DHLA)-PEG-OCH_3-QDs, we wanted to probe their ability to self-assemble with His_6-labeled NLS peptides, and whether the resulting bioconjugates stay aggregate-free *in vitro* and in a live cell system. His-driven self-assembly between QDs and biomolecules requires direct access to the Zn-rich QD surface, and the strongly binding new ligands may interfere with these direct interactions.[43,44]

The NLS peptide we utilized was derived from the Simian virus 40 (SV40) large T-antigen and is structurally similar to the commercial Pep-1 peptide (a common noncovalent carrier of peptides, proteins, and nucleic acids into cells).[37] Figure 6 shows a side-by-side comparison between dispersions of DHLA-PEG-OCH_3-capped QDs and bis(DHLA)-PEG-OCH_3-capped QDs self-assembled with increasing NLS peptide-to-QD molar ratios. Data show that at high peptide concentrations (at NLS:QD molar ratios exceeding 25:1), aggregation combined with a partial loss of the QD PL is observed after 30 min when DHLA-PEG-OCH_3-capped QDs were used (see white arrow in Figure 6A); aggregation was also observed when conjugates

(37) Delehanty, J. B.; Mattoussi, H.; Medintz, I. L. *Anal. Bioanal. Chem.* **2009**, *393*, 1091–1105.
(38) Zanta, M. A.; Belguise-Valladier, P.; Behr, J. P. *Proc. Natl. Acad. Sci. U.S.A.* **1999**, *96*, 91–96.
(39) Tkachenko, A. G.; Xie, H.; Coleman, D.; Glomm, W.; Ryan, J.; Anderson, M. F.; Franzen, S.; Feldheim, D. L. *J. Am. Chem. Soc.* **2003**, *125*, 4700–4701.
(40) Rozenzhak, S. M.; Kadakia, M. P.; Caserta, T. M.; Westbrook, T. R.; Stone, M. O.; Naik, R. R. *Chem. Commun.* **2005**, 2217–2219.
(41) Xu, C. J.; Xie, J.; Kohler, N.; Walsh, E. G.; Chin, Y. E.; Sun, S. H. *Chem. Asian J.* **2008**, *3*, 548–552.
(42) Xie, W.; Wang, L.; Zhang, Y. Y.; Su, L.; Shen, A. G.; Tan, J. Q.; Hu, J. M. *Bioconjugate Chem.* **2009**, *20*, 768–773.
(43) Delehanty, J. B.; Medintz, I. L.; Pons, T.; Brunel, F. M.; Dawson, P. E.; Mattoussi, H. *Bioconjugate Chem.* **2006**, *17*, 920–927.
(44) Sapsford, K. E.; Pons, T.; Medintz, I. L.; Higashiya, S.; Brunel, F. M.; Dawson, P. E.; Mattoussi, H. *J. Phys. Chem. C* **2007**, *111*, 11528–11538.

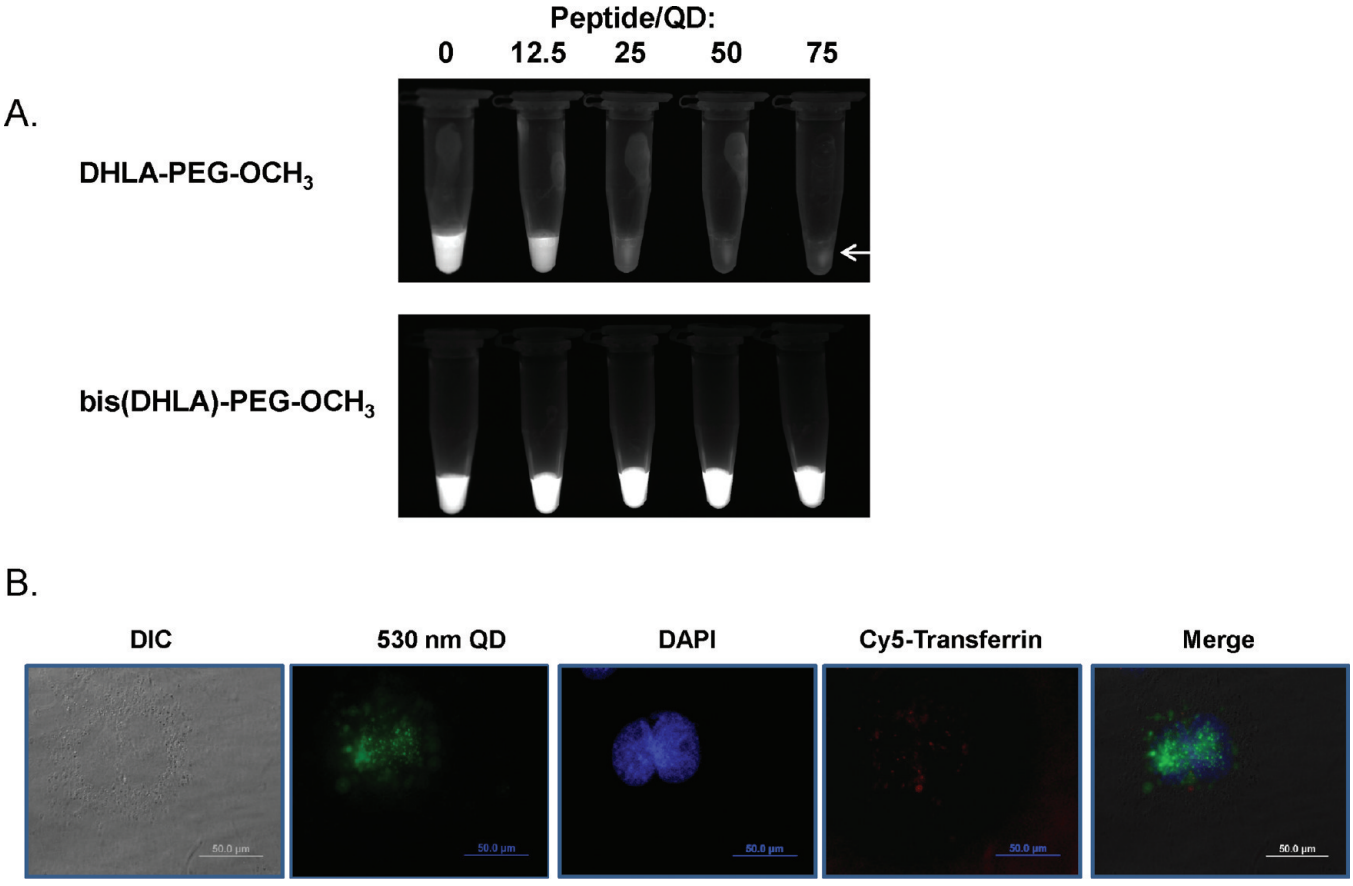

Figure 6. (A) Fluorescent images of DHLA-PEG-OCH_3- and bis(DHLA)-PEG-OCH_3-capped QDs (λ_{em} = 530 nm) self-assembled with the indicated molar ratios of NLS peptide after 30 min at room temperature. The white arrow indicates the presence of aggregated/precipitated QDs. (B) Representative images of COS-1 cells incubated with ~100 nM QD−NLS conjugates. Shown are a DIC image along with the fluorescence images at the 530 nm QD, DAPI, Cy5-transferrin emissions; the merged fluorescence image is shown on the right panel.

were incubated with live cells. The sample with 12.5 equiv of peptide per QD shows visible turbidity as well. In contrast, the dispersions of bis(DHLA)-PEG-OCH_3-capped QDs remained homogeneous and aggregate-free at all molar ratios of peptide used after 2 days.

We then tested the capacity of these peptides to facilitate uptake of QD-NLS conjugates by COS-1 cells. Figure 6B shows three spectrally resolved fluorescence images collected from a typical representative cell at the 530 nm QDs, Cy5-transferrin, and DAPI emission windows, respectively, together with the corresponding merged image; the DIC image of the cell culture is also shown. The images show that the QD distribution within the cells is perinuclear as indicated by the green fluorescence pattern around the nucleus. The QD fluorescence distribution is consistent with that of the endosomes as indicated by the co-localization with Cy5-labeled transferrin signal. However, there is no evidence of QD localization in the nucleus. This result indicates that following uptake the QD-NLS bioconjugates are essentially confined within the endosomes and unable to escape and ultimately enter the nucleus. Such result is consistent with the inability of AuNP-NLS conjugates and other QD-CPP conjugates to escape endosomal compartments, when intracellular uptake is driven by receptor-mediated endocytosis.[39] The *in vitro* and intracellular tests indicate that QDs capped with bis(DHLA)-PEG-OCH_3 ligands provide stable platforms for assembling NLS peptides. The improved integrity of QD-NLS bioconjugates imparted by bis(DHLA)-PEG-OCH_3 suggests that QDs capped with higher coordination PEGylated ligands provide more stable platforms for assembling other peptides and proteins. The interaction of polyhistidine-appended peptides and proteins with QD surfaces coated with DHLA-based ligands and how the dithiol ligands are affected by the polyhistidine coordination is complex, and a complete understanding is still lacking. As such, we tentatively speculate that the improvement in stability of QD-NLS peptide conjugates realized with the bis(DHLA)-PEG-capped QDs is attributed to the reduced effective number of peptides self-assembled on individual QDs. His-driven self-assembly of peptides on the nanocrystal may impose a rearrangement of the ligand structure and density, which could destabilize the nanocrystals and, in this case, may be exacerbated by the highly charged (positive) NLS peptide. Such rearrangements will likely be more extensive with weaker binding ligands (e.g., monothiol-appended ligands) and less extensive with DHLA-PEG, but minimal with the multidentate bis(DHLA)-PEG ligands. Thus, the bis(DHLA)-PEG ligands allow controlled self-assembly of NLS peptides on the QDs, producing stable and aggregate-free conjugates, as shown in the present set of data.

Conclusion

We have reported the design, synthesis, and characterization of a new set of PEG-based ligands with multi-thiol anchoring groups, using simple branching strategies (i.e., Michael addition) followed by DCC coupling reaction. These ligands were designed to chelate to the surface of nanocrystals (QDs and AuNPs) and provide improved colloidal stability. The ligands

yielded water-compatible nanocrystals with remarkable, long-term colloidal stability in buffers from pH ~1.1 to pH ~13.9. Furthermore, the resulting nanocrystals were extremely resistant to aggregation, even in the presence of excess DTT (1.5 M). We also described a preliminary demonstration for the potential utility of such nanocrystals by testing their ability to self-assemble with His_6-appended NLS peptides, often used for the transfection of protein and DNA inside cells, followed by cellular delivery of the QD bioconjugates without visible signs of aggregation. The enhanced nanocrystal stability afforded by the new ligands will allow effective use of these nanoprobes in stringent conditions such as extreme pHs and high salt concentrations and in the presence of excess thiol-containing molecules (e.g., DTT) in biological media. Our future work will focus on further expanding the design to prepare end-functionalized multidentate ligands that can be conjugated to biomolecules and other target entities via covalent coupling.

Acknowledgment. We acknowledge NRL, Office of Naval Research (ONR), DTRA basic research for financial support. M.H.S acknowledges a National Research Council Fellowship through the Naval Research Laboratory. We also thank Dorothy Farrell for assistance with some experimental details.

Supporting Information Available: Experimental details describing the synthesis of **2**−**5**, cap exchange applied to QDs and AuNPs, pH stability tests for both types of NPs, DTT competition tests, peptide conjugation to QDs, cell culture preparations, NMR spectra of **2** and **3**, TEM images of AuNPs after cap exchange with the bis(TA)-PEG-OCH_3 ligands, and fluorescence images of bis(DHLA)-PEG-capped QDs in the presence of added NaCl. This material is available free of charge via the Internet at http://pubs.acs.org.

JA102898D